

Preparation and characterization of mesoporous MO_2 ($\text{M} = \text{Ti}, \text{Ce}, \text{Zr}, \text{and Hf}$) nanopowders by a modified sol–gel method

Sorapong Pavasupree^a, Yoshikazu Suzuki^a, Sommai Pivsa-Art^b, Susumu Yoshikawa^{a,*}

^a*Institute of Advanced Energy, Kyoto University, Uji, Kyoto 611-0011, Japan*

^b*Department of Materials and Metallurgical Engineering, Faculty of Engineering,
Rajamangala Institute of Technology, Klong 6, Pathumthani 12110, Thailand*

Received 25 August 2004; received in revised form 29 September 2004; accepted 12 October 2004

Available online 13 January 2005

Abstract

Mesoporous high surface area and high crystallinity MO_2 powders (TiO_2 , CeO_2 , ZrO_2 , and HfO_2) were synthesized by a modified sol–gel method using laurylamine hydrochloride, metal alkoxide and acetylacetone. The prepared MO_2 powders, characterized by XRD, nitrogen adsorption isotherm, SEM, TEM, and SAED, had crystalline size of about 5–15 nm, specific surface area of 44–80 m^2/g , and a narrow pore size distribution with average pore diameter of about 3–6 nm. This synthesis method provides a new simple route to fabricate nanostructured materials under mild conditions.

© 2004 Elsevier Ltd and Techna Group S.r.l. All rights reserved.

Keywords: Mesoporous oxides; Characterization; Sol–gel; Mild conditions

1. Introduction

Metal oxides with wide or moderate band gap, such as TiO_2 , CeO_2 , ZrO_2 , and HfO_2 , have been widely used for various applications like semiconductor materials in dye-sensitized solar cell, catalysts, fuel cells, resistors, gas sensors, transparent optical device, and optical coatings [1–8]. Their functional properties are influenced by many factors such as crystallinity, particle size, surface area, and preparation [8–13]. In previous works, mesoporous TiO_2 -based nanopowders with pore size about 5 nm were synthesized by a modified sol–gel method in aqueous phase using a surfactant-assisted process, offering a high photocatalytic activity [11]. This process has also been applied to a semiconductive material in dye-sensitized solar cells [12–15].

In this study, the surfactant-assisted process has been expanded to prepare other metal oxides. Mesoporous CeO_2 , ZrO_2 , HfO_2 , as well as TiO_2 were synthesized using

laurylamine hydrochloride (LAHC)/metal alkoxide modified with acetylacetone (ACA) system. The nanopowders characteristics will be reported.

2. Experimental

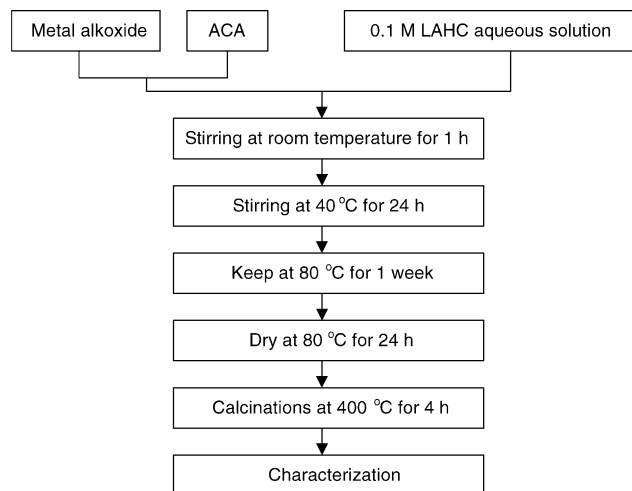
For mesoporous TiO_2 preparation, tetraisopropylorthotitanate (TIPT, Tokyo Chemical Industry Co., Ltd.) was mixed with the same mole of ACA (Nacalai Tesque, Inc.) to slowdown the hydrolysis and the condensation reactions [11–13]. Subsequently, 0.1 M LAHC (Tokyo Chemical Industry Co.) aqueous solution (as the surfactant, pH 4–4.5) was added in the solution (molar ratio of TIPT to LAHC was 4), and it was stirred at room temperature for 1 h. After kept stirring at 40 °C for 24 h, it was put into an oven at 80 °C for 1 week. The alcohol by-product was removed by drying at 80 °C for 24 h, followed by calcinations at 400 °C for 4 h (Fig. 1). Mesoporous CeO_2 , ZrO_2 , and HfO_2 nanopowders were synthesized using the same route of TiO_2 by changing alkoxide precursors (Table 1).

* Corresponding author. Tel.: +81 774 38 3502; fax: +81 774 38 3508.
E-mail address: s-yoshi@iae.kyoto-u.ac.jp (S. Yoshikawa).

Table 1

Physicochemical properties of the prepared metal oxides calcined at 400 °C for 4 h

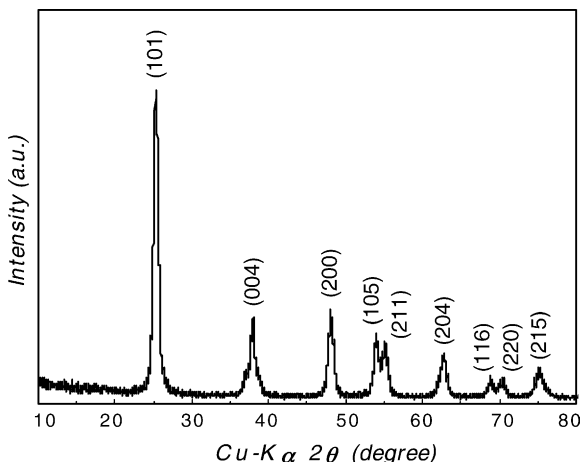
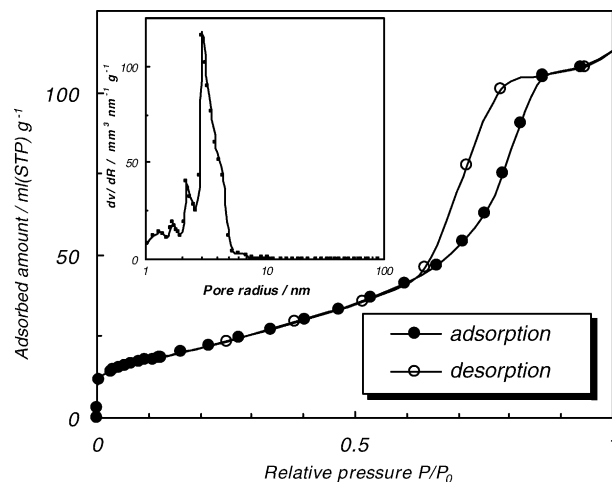
Oxide	Inorganic precursor	Crystalline structure	Crystalline size (nm)	Pore size (nm)	Pore volume (cm ³ /g)	Surface area (m ² /g)
TiO ₂	Ti(OCH(CH ₃) ₂) ₄	Tetragonal (anatase)	7–15	5–6	0.197	80
CeO ₂	Ce(O(CH ₂) ₃ CH ₃) ₄	Cubic (fluorite-type)	5–10	3–4	0.113	73
ZrO ₂	Zr(O(CH ₂) ₃ CH ₃) ₄	Tetragonal	7–15	3–4	0.063	72
HfO ₂	Hf(O(CH ₂) ₃ CH ₃) ₄	Monoclinic	7–15	3–5	0.057	44



Condition: [Metal alkoxide] / [ACA] = 1, [Metal alkoxide] / [LAHC] = 4

Fig. 1. Flow sheet of processing steps.

The crystalline structure of samples was evaluated by X-ray diffraction (XRD, RIGAKU RINT 2100). The microstructure of the prepared materials was analyzed by scanning electron microscopy (SEM, JEOL JSM-6500FE), transmission electron microscopy (TEM, JEOL JEM-200CX), and selected-area electron diffraction (SAED). The nitrogen adsorption isotherm and Brunauer–Emmett–Teller (BET) specific surface area of materials, which were outgassed overnight at 200 °C, were measured with BEL Japan BELSORP-18 Plus equipment.

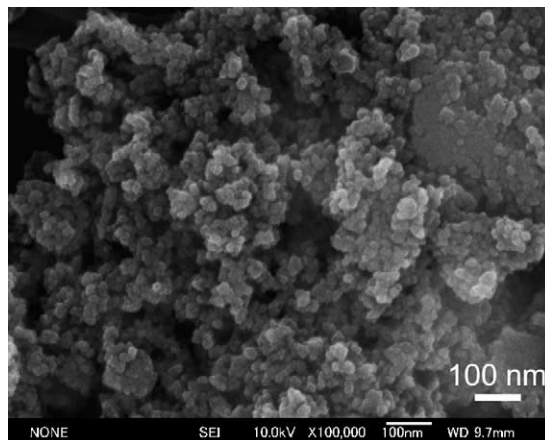
Fig. 2. X-ray diffraction pattern of TiO₂ calcined at 400 °C for 4 h.Fig. 3. Nitrogen adsorption isotherm pattern of TiO₂ calcined at 400 °C for 4 h, and the pore size distribution of sample with pore diameter about 5–6 nm (inset).

3. Results and discussion

3.1. Mesoporous TiO₂

The X-ray diffraction pattern of the TiO₂ sample calcined at 400 °C for 4 h, demonstrated the formation of anatase phase as shown in Fig. 2. The peaks were rather sharp, which indicated relatively high crystallinity.

Fig. 3 gives the nitrogen adsorption isotherm of the TiO₂ sample calcined at 400 °C for 4 h, which shows a typical

Fig. 4. SEM image of TiO₂ calcined at 400 °C for 4 h.

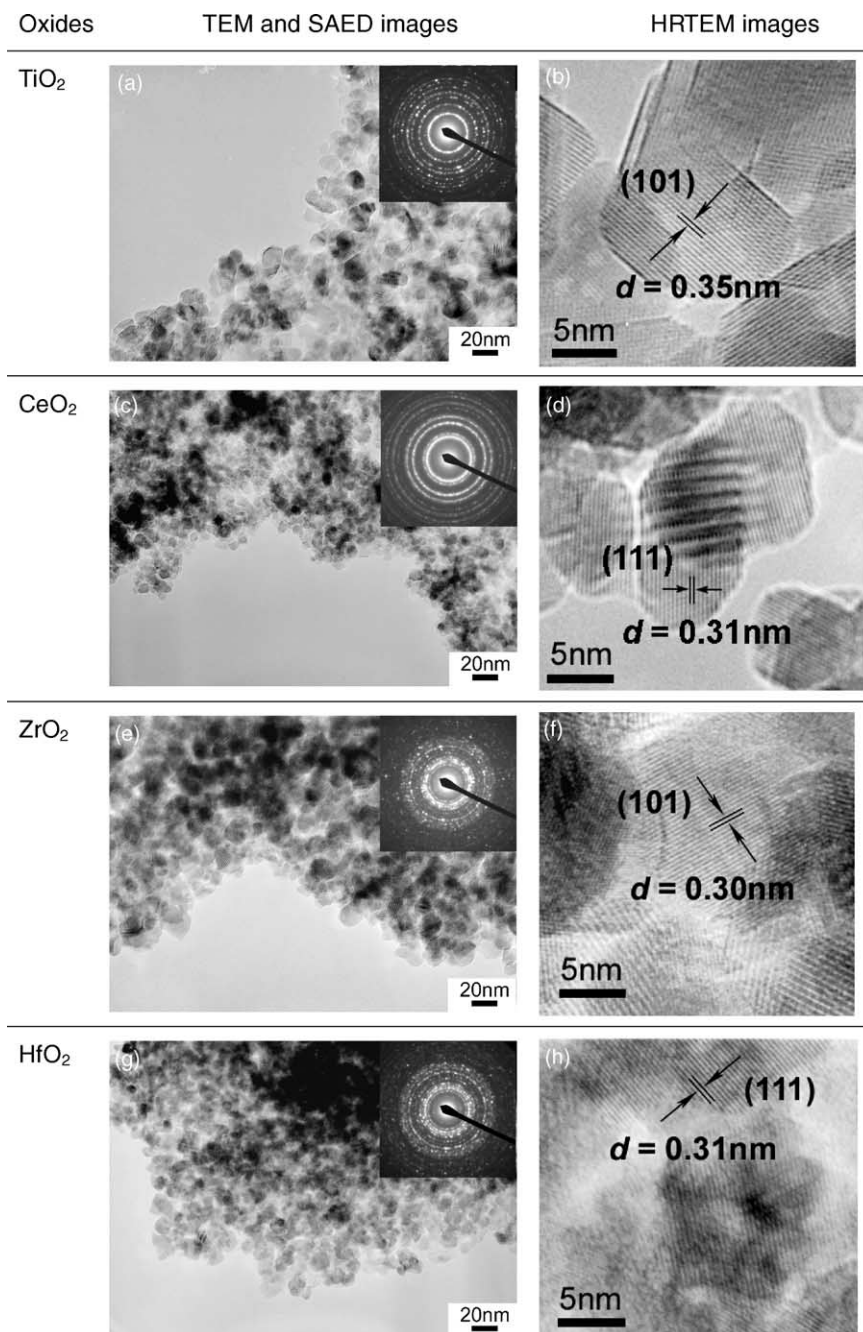


Fig. 5. TEM, SAED, and HRTEM images of the prepared metal oxides.

IUPAC type IV pattern, indicating the existence of mesopores. The pore size distribution of the sample (inset of Fig. 3) showed that the prepared material was mesoporous with narrow pore size distribution (average pore diameter about 5–6 nm). The BET surface area and pore volume of sample are about 80 m²/g and 0.197 cm³/g, respectively.

Fig. 4 shows a representative SEM image of TiO₂ calcined at 400 °C for 4 h. The image indicates spherical nature of the particles, with larger particles being aggregates of the smaller ones. TEM image of the same powder,

Fig. 5(a), shows a 7–15 nm nano-size crystalline structure. The SAED pattern (inset of Fig. 5(a)) and high resolution TEM image (Fig. 5(b)) demonstrated that the nanoparticles consisted of the anatase phase.

3.2. Mesoporous CeO₂ and other metal oxides

The XRD pattern of the CeO₂ sample calcined at 400 °C for 4 h showed peaks corresponding to the cubic fluorite structure (Fig. 6).

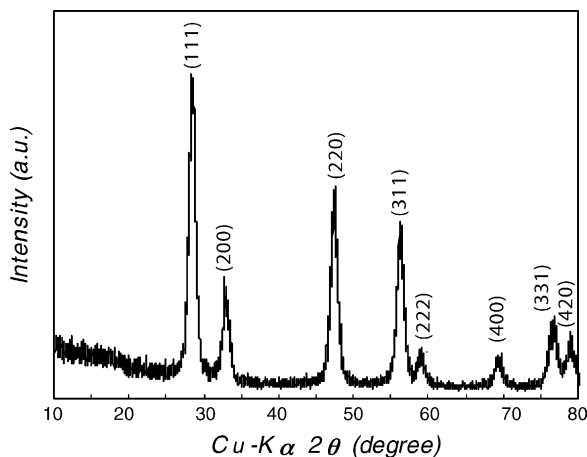


Fig. 6. X-ray diffraction pattern of CeO₂ calcined at 400 °C for 4 h.

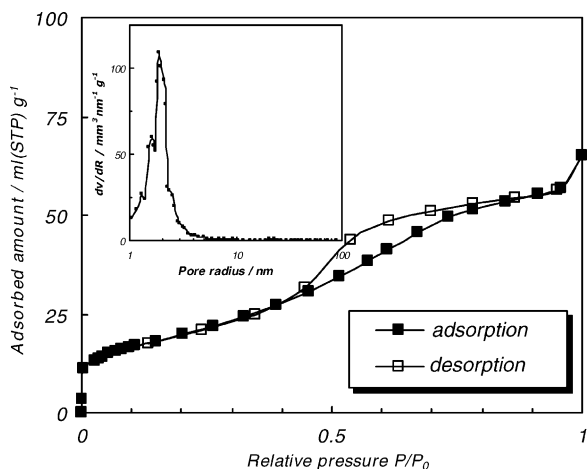


Fig. 7. Nitrogen adsorption isotherm pattern of CeO₂ calcined at 400 °C for 4 h, and the pore size distribution of sample with pore diameter about 3–4 nm (inset).

Fig. 7 gives the nitrogen adsorption isotherm of the same CeO₂ sample. The isotherm also showed an IUPAC type IV, as that of TiO₂, and the pore size distribution (inset of Fig. 7) was about 3–4 nm. The BET surface area and pore volume of sample are about 73 m²/g and 0.113 cm³/g, respectively.

TEM image of the CeO₂ nanopowder (Fig. 5(c)) had crystal size about 5–10 nm. The SAED pattern (inset of Fig. 5(c)) and high resolution TEM image (Fig. 5(d)) showed that the nanoparticles were composed of cubic fluorite type CeO₂.

ZrO₂ and HfO₂, mesoporous nanopowders were also successfully obtained by the modified sol–gel method. The nanopowders calcined at 400 °C for 4 h were composed of tetragonal ZrO₂ and monoclinic HfO₂, having mesopores of 3–5 nm. BET surface area of ZrO₂ and HfO₂ was about 72 and 44 m²/g, respectively (Table 1). The particles of these metal oxides are spherical in nature, with crystalline size about 7–15 nm (Fig. 5(e)–(h)).

4. Conclusions

The modified sol–gel process using a surfactant enabled to fabricate various metal oxides with controlled mesopores. All products possessed high crystallinity with crystal size about 5–15 nm, high surface area (44–80 m²/g), and average pore diameter about 3–6 nm. These materials are promising for chemical and energy-related applications such as photocatalysts, and semiconductors in dye-sensitized solar cell.

Acknowledgements

The authors would like to express gratitude to Prof. S. Isoda and Prof. H. Kurata, Institute for Chemical Research, Kyoto University for the use of TEM apparatus and Prof. T. Yoko, Institute for Chemical Research, Kyoto University for the use of XRD equipment. Cerium butoxide, zirconium butoxide, and hafnium butoxide were kindly supplied by Hokko Chemical Industry Co., Ltd. This work was supported by a grant-in-aid from the Ministry of Education, Science Sports, and Culture of Japan under the 21 COE program and the Nanotechnology Support Project.

References

- [1] M. Grätzel, Photoelectrochemical cells, *Nature* 414 (2001) 338–344.
- [2] A. Fujishima, T.N. Rao, D.A. Tryk, Titanium dioxide photocatalysis, *J. Photochem. Photobiol. C: Photochem. Rev.* 1 (2000) 1–21.
- [3] E. Bekyarova, P. Fornasiero, J. Kaspar, M. Graziani, CO oxidation on Pd/CeO₂–ZrO₂ catalysts, *Catal. Today* 45 (1998) 179–183.
- [4] M. Gilo, N. Croitoru, Study of HfO₂ films prepared by ion-assisted deposition using a gridless end-hall ion source, *Thin Solid Films* 350 (1999) 203–208.
- [5] M. Alvisi, M. Di Giulio, S.G. Marrone, M.R. Perrone, M.L. Protopapa, A. Valentini, L. Vasanelli, HfO₂ films with high laser damage threshold, *Thin Solid Films* 358 (2000) 250–258.
- [6] M. Maczka, E.T.G. Lutz, H.J. Verbeck, K. Oskam, A. Meijerink, J. Hanuza, J. Stuijvinga, Spectroscopic studies of dynamically compacted monoclinic ZrO₂, *J. Phys. Chem. Solids* 60 (1999) 1909–1914.
- [7] S. Park, J.M. Vohs, R.J. Gorte, The direct oxidation of hydrocarbons in a solid oxide fuel cell, *Nature* 404 (2000) 265–267.
- [8] F. Zhang, S. Yang, H. Chen, X. Yu, Preparation of discrete nanosize ceria powder, *Ceram. Int.* 30 (2004) 997–1002.
- [9] C.C. Wang, J.Y. Ying, Sol–gel synthesis and hydrothermal processing of anatase and rutile titania nanocrystals, *Chem. Mater.* 11 (1999) 3113–3120.
- [10] K. Ishizaki, S. Komarneni, M. Nanko, *Porous Materials Process Technology and Applications*, Kluwer Academic Publishers, 1998, Chapters 1, 4, 5.
- [11] M. Adachi, Y. Murata, M. Harada, S. Yoshikawa, Formation of titania nanotubes with high photo-catalytic activity, *Chem. Lett.* 8 (2000) 942–943.
- [12] M. Adachi, I. Okada, S. Ngamsinlapasathian, Y. Murata, S. Yoshikawa, Dye-sensitized solar cell using semiconductor thin film composed of titania nanotubes, *Electrochemistry* 70 (2002) 449–452.
- [13] M. Adachi, Y. Murata, I. Okada, S. Yoshikawa, Formation of titania nanotubes and applications for dye-sensitized solar cells, *J. Electrochem. Soc.* 150 (8) (2003) G488–G493.

- [14] S. Ngamsinlapasathian, S. Sakulhaemaruehai, S. Pavasupree, A. Kitiyanan, T. Sreethawong, Y. Suzuki, S. Yoshikawa, Highly efficient dye-sensitized solar cell using nanocrystalline titania containing nanotube structure, *J. Photochem. Photobiol. A* 164 (2004) 145–151.
- [15] S. Ngamsinlapasathian, T. Sreethawong, Y. Suzuki, S. Yoshikawa, Single and double layered mesoporous $\text{TiO}_2/\text{P25}$ TiO_2 electrode for dye-sensitized solar cell, *Sol. Energy Mater. Sol. Cells*, in press.